



Research Article

CPT1A mediates chemoresistance in human hypopharyngeal squamous cell carcinoma via ATG16L1-dependent cellular autophagy



Lianhui Sun^{b,*}, Xing Wang^{c,1}, Lixiao Chen^{a,1}, Zheng Gao^d, Songhui Xu^e, Chen Hu^b,
Guangjian Fan^b, Baoxin Wang^a, Tingting Feng^{f,**}, Wang Wang^{g,***}, Xinjiang Ying^{a,****}

^a Department of Otolaryngology Head and Neck Surgery, Shanghai General Hospital, Shanghai Jiaotong University School of Medicine, Shanghai, 201620, China

^b Precision Research Center for Refractory Diseases, Institute for Clinical Research, Shanghai General Hospital, Shanghai Jiao Tong University School of Medicine, Shanghai, 200080, China

^c Jiangxi Provincial People's Hospital, The First Affiliated Hospital of Nanchang Medical College, Nanchang, China

^d State Key Laboratory of Protein and Plant Gene Research, Peking-Tsinghua Center for Life Sciences, School of Advanced Agriculture Sciences, Peking University, Beijing, 100871, China

^e Department of Urology, The First Affiliated Hospital of Nanchang University, Nanchang, China

^f Department of Clinical Pharmacy, Shanghai General Hospital, Shanghai Jiao Tong University School of Medicine, Shanghai, China

^g School of Cell and Gene Therapy, Shanghai Jiaotong University School of Medicine, Shanghai, 201600, China

HIGHLIGHTS

- The overexpression of CPT1A contributes to HSCC chemoresistance.
- CPT1A interacts with and stimulate the succinylation of ATG16L1, which in turn drives autophagy.
- The CPT1A inhibitor significantly enhances cisplatin sensitivity both in vitro and in vivo.

ABSTRACT

Hypopharyngeal squamous cell carcinoma (HSCC) is a highly aggressive malignancy that constitutes approximately 95% of all hypopharyngeal carcinomas, and it carries a poor prognosis. The primary factor influencing the efficacy of anti-cancer drugs for this type of carcinoma is chemoresistance. Carnitine palmitoyltransferase 1A (CPT1A) has been associated with tumor progression in various cancers, including breast, gastric, lung, and prostate cancer. The inhibition or depletion of CPT1A can lead to apoptosis, curbing cancer cell proliferation and chemoresistance. However, the role of CPT1A in HSCC is not yet fully understood. In this study, we discovered that CPT1A is highly expressed in HSCC and is associated with an advanced T-stage and a poor 5-year survival rate among patients. Furthermore, the overexpression of CPT1A contributes to HSCC chemoresistance. Mechanistically, CPT1A can interact with the autophagy-related protein ATG16L1 and stimulate the succinylation of ATG16L1, which in turn drives autophagosome formation and autophagy. We also found that treatment with 3-methyladenine (3-MA) can reduce cisplatin resistance in HSCC cells that overexpress CPT1A. Our findings also showed that a CPT1A inhibitor significantly enhances cisplatin sensitivity both in vitro and in vivo. This study is the first to suggest that CPT1A has a regulatory role in autophagy and is linked to poor prognosis in HSCC patients. It presents novel insights into the roles of CPT1A in tumorigenesis and proposes that CPT1A could be a potential therapeutic target for HSCC treatment.

1. Introduction

Hypopharyngeal squamous cell carcinoma (HSCC), an aggressive malignancy originating from the upper aerodigestive tract, has the poorest prognosis among head and neck cancers (Kwon et al., 2019).

Chemotherapy is a primary modality for HSCC adjuvant therapy. Induction chemotherapy, using drugs such as docetaxel, 5-fluorouracil, and cisplatin, has significantly improved HSCC outcomes (Lian et al., 2017; Pointreau et al., 2009; Vermorken et al., 2007). Nevertheless, chemoresistance is the major dilemmas to influence the effects of these

* Corresponding author.

** Corresponding author.

*** Corresponding author.

**** Corresponding author.

E-mail addresses: sunlianhui2009@126.com (L. Sun), ycttfeng@163.com (T. Feng), echowangwang0901@126.com (W. Wang), yingxinjiang@126.com (X. Ying).

¹ These authors contributed equally to this work.

anti-cancer drugs (Wilson et al., 2006), resulting in a low survival rate and overall poor prognosis of HSCC. Chemoresistance can be occurred by different mechanisms, including DNA repair, mitochondrial dynamics alteration, epithelial-mesenchymal transition (EMT), cancer stemness, tumor-derived exosome and autophagy induction (Luqmani, 2005; Mansoori et al., 2017; Sui et al., 2013). The in-depth investigation into the molecular mechanisms of chemoresistance is necessary and hopeful to identify new targets for HSCC therapy.

Autophagy is a highly conserved catabolic process that sequesters damaged or redundant proteins, organelles, or other cytoplasmic components via autophagic vacuoles (Aves), transporting them to the lysosomal system for degradation (Pu et al., 2016). This process involves several conserved autophagy-related (ATG) proteins. The microtubule-associated protein 1 light chain 3 (LC3) is cleaved by ATG4 to form cytoplasmic LC3-I, which is subsequently activated by ATG7, transferred to ATG3, and conjugated to phosphatidylethanolamine (PE) (Hemelaar et al., 2003; Tanida et al., 2001, 2002). The transfer reaction of LC3 from ATG3 to PE (resulting in LC3-II) is facilitated by the ATG12-ATG5-ATG16L1 complex, which determines the site of LC3-II production (Fujita et al., 2008). The number of autophagosomes correlates with LC3-II levels and LC3 vesicle numbers, serving as indicators of the autophagic level. It is generally believed that autophagy is significantly induced by several chemotherapy drugs and plays a critical role in the chemoresistance processes of various tumor types, such as glioma, osteosarcoma, gastric cancer, and acute myeloid leukemia (Poillet-Perez et al., 2021; Xiao et al., 2018; Xu et al., 2020; Yan et al., 2016).

Autophagy acts as a defense mechanism, allowing cancer cells to adapt and survive under energy-deprived conditions induced by chemotherapy (Galluzzi et al., 2015; White, 2015). Chemotherapeutic drugs primarily target rapidly dividing cancer cells, causing cellular stress and autophagy activation. Autophagy recycles intracellular components to generate nutrients and energy, enabling cancer cells to combat the energy deprivation induced by chemotherapy. This adaptive response ultimately encourages cell survival and proliferation, resulting in resistance to chemotherapy drugs. Furthermore, autophagy can contribute to chemotherapy resistance by inducing autophagic cell death, a type of programmed cell death characterized by excessive activation of the autophagy pathway (Sui et al., 2013; White et al., 2009). In some scenarios, cancer cells utilize autophagy as an alternate pathway for cell death, evading apoptosis, which is the primary target of chemotherapy. This allows them to bypass the cytotoxic effects of chemotherapy drugs and develop resistance. It's critical to understand the mechanisms that connect the induction of autophagy and resistance to chemotherapy in order to improve cancer treatment strategies. Targeting processes related to autophagy could provide a promising way to boost the effectiveness of chemotherapy and overcome resistance. Previous studies have shown that autophagic proteins, such as Beclin-1 and LC3-II, are under-expressed in HSCCs, and their abnormal expression is associated with a poor prognosis for HSCCs (Wang et al., 2013). However, it remains unclear whether autophagy impacts the sensitivity of HSCC to chemotherapeutic drugs. CPT1A, a subtype of the carnitine palmitoyl transferase 1 (CPT1) transport system, catalyzes the formation of acylcarnitine from long-chain acyls and carnitine. It is the crucial rate-limiting enzyme in fatty acid oxidation (FAO) (Qu et al., 2016). Considering that abnormal fatty acid oxidation (FAO) is a characteristic of tumor metabolic reprogramming, targeting CPT1A may prove beneficial for radiation therapy in patients with nasopharyngeal carcinoma (NPC) and breast cancer (Tan et al., 2018, 2021; Xiong, 2018). Recent studies have demonstrated that CPT1A possesses lysine succinyltransferase (LSTase) activity, both in vitro and in vivo. A proteomics approach, based on stable isotope labeling by amino acids in cell culture (SILAC), revealed that 101 proteins were more succinylated in cells expressing wild-type (WT) CPT1A than in cells with the control vector (Kurmi et al., 2018). Succinylation of S100A10 by CPT1A promotes gastric cancer progression (Wang et al., 2019). CPT1A involves in ovarian cancer progression through MFF succinylation (Shao et al., 2022). These reports imply that

CPT1A could be a potential target for tumor therapy. However, its potential role in HSCC has not yet been explored.

In this study, we demonstrate that CPT1A is highly expressed and correlated with poor prognosis in HSCC patients. CPT1A interacts with and succinylates ATG16L, thereby promoting autophagy through the ATG12-ATG5-ATG16L1 interaction. Significantly, treatment with the PI3K inhibitor 3-methyladenine (3-MA) reduces cisplatin resistance in HSCC cells overexpressing CPT1A. Moreover, the use of a CPT1A inhibitor significantly enhances cisplatin sensitivity both in vitro and in vivo. Overall, these results reveal the molecular mechanism by which CPT1A promotes the autophagy process in HSCC, providing novel insights into the role of CPT1A in HSCC tumorigenesis.

2. Results

2.1. CPT1A is highly expressed in human HSCC patients and correlated with poor prognosis

To determine if CPT1A plays a crucial role in the progression of HSCC, we conducted an immunohistochemistry (IHC) analysis to measure the CPT1A expression level in 19 human HSCC samples. The CPT1A protein exhibited higher expression in the majority of clinical HSCC samples as compared to the peri-tumor tissues from the same 19 patients (Fig. 1A–B). To further validate the expression of CPT1A, we performed RT-qPCR and Western blot (WB) analysis on matched peri-tumor tissues and HSCC tissues from three distinct patients. All of the carcinoma tissues displayed significant expression of CPT1A mRNA and protein, while the peri-tumor tissues exhibited low CPT1A expression at the mRNA and protein levels (Fig. 1C–D). We also evaluated the relationship between CPT1A expression and the clinicopathological characteristics of 83 HSCC patients. As depicted in Fig. 1E, HSCC patients with elevated CPT1A expression had worse overall survival rates than those with lower CPT1A expression. To understand the clinical significance of CPT1A alterations in HSCC, we examined the expression levels of each CPT1A gene at various stages of TCGA HSCC samples. We discovered that CPT1A was significantly overexpressed in advanced-stage HSCC (Fig. 1F). These findings suggest that CPT1A may play a pivotal role in the development of HSCC and could be a valuable predictive marker for poor prognosis in HSCC.

2.2. High expression of CPT1A promotes chemoresistance in human HSCC

Induction chemotherapy using docetaxel, 5-fluorouracil, and cisplatin has been developed as an alternative to total laryngectomy. This approach has significantly improved outcomes for HSCC (Lian et al., 2017; Pointreau et al., 2009; Vermorken et al., 2007). However, multi-drug resistance (MDR) is a primary factor in chemotherapy failure and contributes significantly to increased cancer-related mortality (Holohan et al., 2013). To investigate the relationship between CPT1A and MDR, we measured CPT1A levels during chemotherapeutic drug treatment. Interestingly, we found that the CPT1A protein level, rather than the mRNA level, significantly increased under treatment with cisplatin, taxol, and 5-FU (Fig. 2A–B). To determine whether the CPT1A protein level influences chemotherapy resistance, we generated a stable cell line with CPT1A knockdown (Fig. 2C). We then performed a time-course cell viability assay using the CCK-8 kit to evaluate the cytotoxic effect of these chemotherapeutic drugs on CPT1A knockdown cells. The results indicated that CPT1A knockdown improves the sensitivity of these cells to chemotherapeutic drugs (Fig. 2D). To confirm the drug sensitivity induced by CPT1A knockdown, we found that rescuing CPT1A expression recovers resistance to chemotherapy drugs (Fig. 2E–F). These results suggest a positive correlation between high CPT1A expression and MDR.

2.3. CPT1A mediates autophagy under cisplatin treatment

Reports suggest that high levels of autophagy often lead to

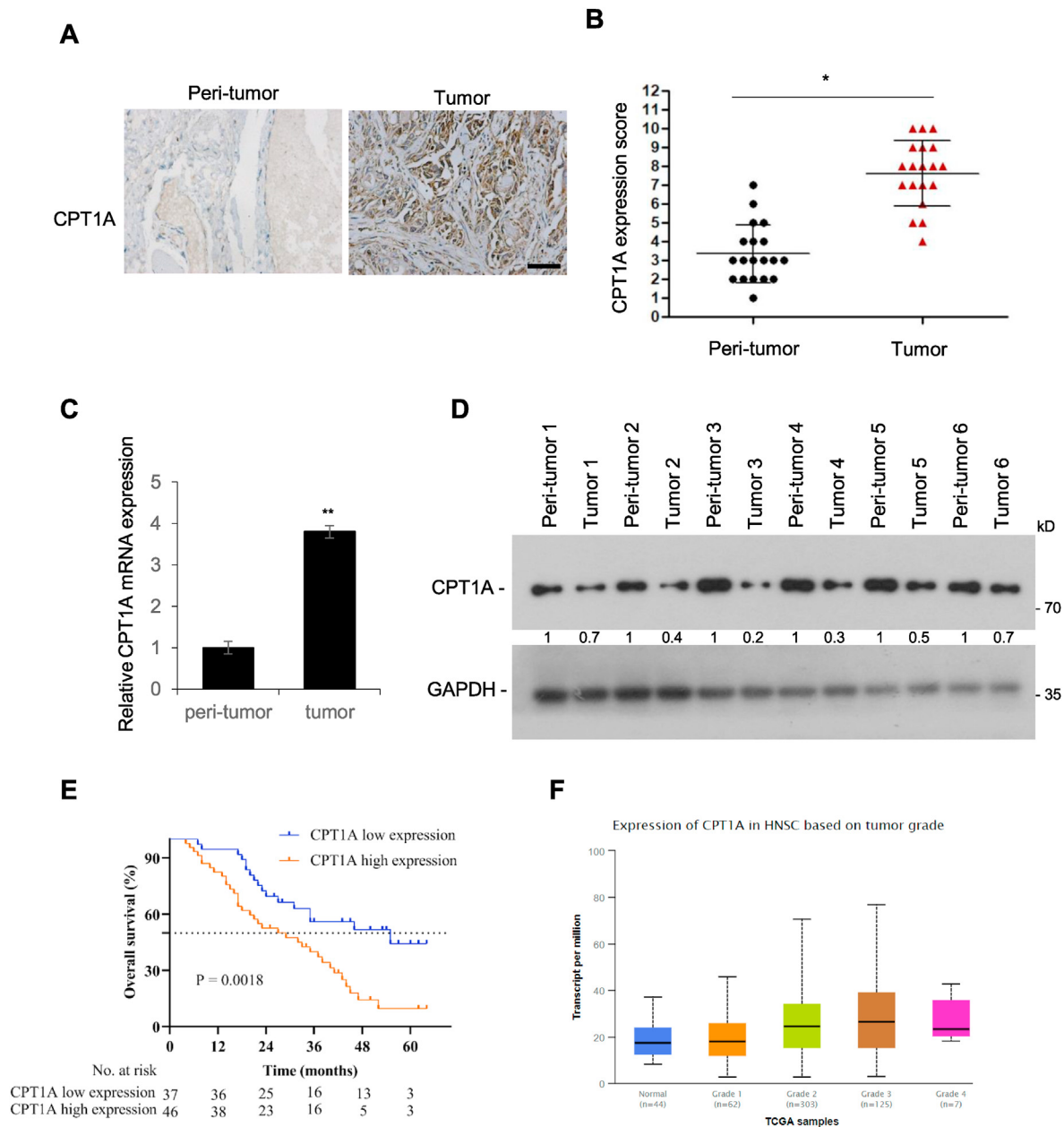


Fig. 1. CPT1A is highly expressed in human HSCC patients and correlated with poor prognosis.

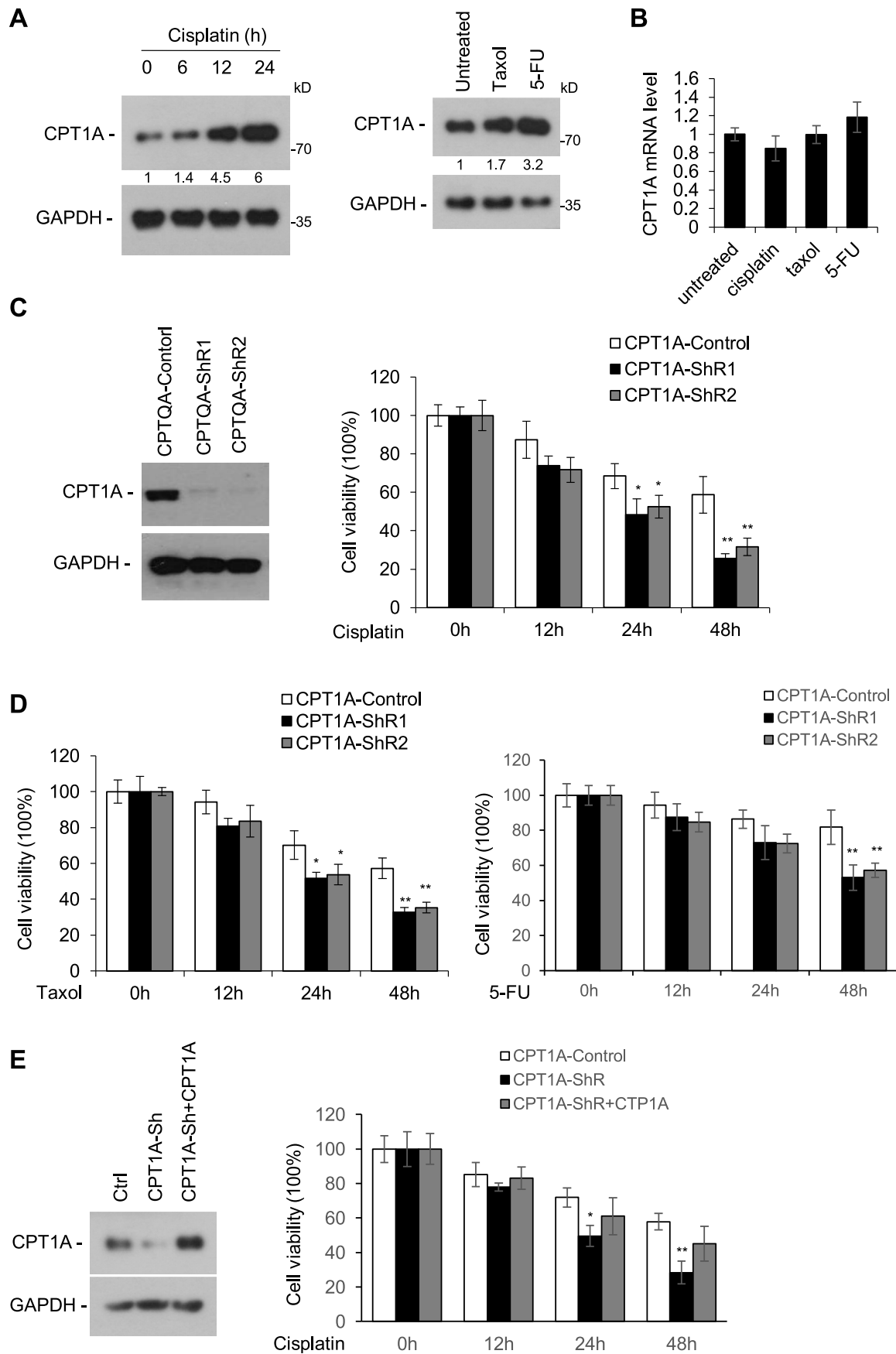
(A) Representative images (40 \times magnification) of IHC staining for CPT1A in HSCC tissues and adjacent normal tissues. T represents tumor tissues; P represents peri-tumor tissues. (B) Relative IHC staining for CPT1A in HSCC tissues and adjacent normal tissues (scale bar, 100 μ m). (C–D) Total mRNAs and proteins were extracted from tissue samples of three individual HSCC patients and were subjected to qPCR (C) and Western blot (D) analysis, respectively. (E) The Kaplan–Meier curve depicts the long-term survival of HSCC patients (n = 83). The curves were stratified based on the CPT1A level scored by intensity (0–3) and the area (0–4) of the staining with TMA and IHC technology. (F) The expression of CPT1A is associated with the tumor stage in HSCC patients. Data represent the mean \pm SD of three independent experiments. * p < 0.05.

chemotherapy insensitivity, a common phenomenon that significantly reduces the therapeutic effect in cisplatin-resistant tumor cells. In line with this, we discovered that chemotherapy drugs trigger autophagy, as evidenced by quantification of GFP-LC3 puncta formation in HSCC cells (Fig. 3A–B). We then evaluated autophagy marker levels via western blotting. We observed a notable increase in LC3-II and a clear decrease in p62 in cells treated with chemotherapy drugs (Fig. 3C). This prompted us to investigate the functional role of CPT1A in autophagy. As anticipated, overexpression of CPT1A led to an increase in GFP-LC3 puncta formation (Fig. 3D–E). Additionally, LC3-II levels increased and p62 levels decreased in cells overexpressing CPT1A (Fig. 3F). To verify the effect of CPT1A on autophagy during chemotherapy drug treatment, we assessed

the autophagy markers in stable CPT1A knockdown cells with or without cisplatin. Cisplatin treatment induced LC3 puncta formation and LC3-II upregulation in control cells but not in CPT1A knockdown cells (Fig. 3G–I). These results suggest that chemotherapeutic drugs induce autophagy in a CPT1A-dependent manner.

2.4. CPT1A interacts with the autophagy-activated genes ATG16L1 and succinylates ATG16L1

To investigate the role of CPT1A in autophagy, we precipitated potential interacting proteins using protein A beads and subjected the sample to mass spectrometry analysis, identifying ATG16L1 (Fig. 4A). We



(caption on next page)

Fig. 2. High expression of CPT1A promotes chemoresistance in human HSCC

(A) Fadu cells were subjected to treatment with cisplatin (10 μ M) for specified durations, and with Taxol (10 nM) and 5-FU (5 μ M) for 48h. The CPT1A protein levels were then detected through western blotting. (B) Fadu cells were treated with cisplatin (10 μ M), Taxol (10 nM), and 5-FU (5 μ M) for 48h. The CPT1A mRNA levels were then detected through a qRT-PCR assay. (C) Cells with CPT1A knockdown were generated and the presence of CPT1A was detected through western blotting. (D) Fadu cells, stably transfected with scrambled shRNA and CPT1A shRNA, were seeded in 96-well plates at a density of 1×10^4 cells/well. After incubating overnight, the culture medium was replaced with a fresh medium containing Taxol, 5-fluorouracil (5-FU), and cisplatin. A control set was also included, in which fresh medium alone was added, without the drugs. Cell viability was detected through a CCK8 assay. (E) Fadu cells with stable CPT1A knockdown (CPT1A-ShR) or a vector control (CPT1A-Control) were treated with cisplatin for specified durations, and cell viability was analyzed through a CCK8 assay. To determine the specific effect of CPT1A, cells with CPT1A knockdown were infected with lentiviral vectors expressing CPT1A. Data represent the mean \pm SD of three independent experiments. * $p < 0.05$, ** $p < 0.01$.

then expressed Flag-CPT1A and GFP-ATG16L1 plasmids in 293T cells to examine their binding with CPT1A, confirming that CPT1A interacts with the autophagy-activated gene, ATG16L1 (Fig. 4B). An endogenous complex of CPT1A and ATG16L1 was also detected in HSCC cells (Fig. 4C). CPT1A has been shown to have lysine succinyltransferase activities (Kurmi et al., 2018), but the physiological significance of lysine succinylation, a relatively new post-translational modification (PTM), in HSCC is not yet clear. Thus, we explored whether CPT1A could succinylate ATG16L1, focusing on the study of succinylation modification in HSCC. Results showed that ATG16L1, when immunoprecipitated, was succinylated by CPT1A (Fig. 4D). Furthermore, *in vitro* enzyme activity experiments demonstrated that CPT1A directly succinylates ATG16L1 (Fig. 4E). Taken together, these results indicate that CPT1A interacts with and succinylates ATG16L1.

2.5. CPT1A induces autophagy through the ATG12-ATG5-ATG16L1 complex under chemotherapeutic drugs treatment

Considering the critical role of ATG12-ATG5-ATG16L1 complex formation in phagophore elongation during autophagy in mammalian cells (Hanada et al., 2007), we investigated the potential involvement of CPT1A in autophagic complex formation. Accordingly, we conducted co-immunoprecipitation experiments and discovered that CPT1A fosters the formation of ATG5-ATG16L1 and ATG12-ATG16L1 complexes within autophagosomes (Fig. 5A–B). To determine whether ATG16 mediates the promotion of autophagy by CPT1A, we examined the effect of CPT1A overexpression and ATG16 silencing on GFP-LC3 puncta. We found that overexpression of CPT1A significantly increased GFP-LC3 puncta, while silencing of ATG16 reversed the upregulation of GFP-LC3 puncta (Fig. 5C–D). Our findings, therefore, suggest that CPT1A promotes autophagosome formation via the ATG12-ATG5-ATG16L1 complex.

To further investigate the interaction between CPT1A and ATG16L1 under the effects of chemotherapeutic drugs, we conducted co-immunoprecipitation experiments. These demonstrated an increase in the association between CPT1A and ATG16L1 upon cisplatin treatment (Fig. 5E). Additionally, cisplatin treatment was found to notably increase ATG16L1 succination (Fig. 5F). We also examined the succination of ATG16L1 induced by cisplatin in cells with CPT1A knocked down. The data showed that cisplatin treatment significantly enhanced ATG16L1 succination in cells with normal CPT1A. However, an increase in ATG16L1 succination in CPT1A knockdown cells was not observed (Fig. 5G). To further investigate whether CPT1A's autophagy induction depends on its palmitoyltransferase or succinyltransferase activity, we created the palmitoyltransferase activity defective mutants, CPT1A-G710E and CPT1A-H473A. Interestingly, it was noted that these mutants, similar to wild-type CPT1A, were able to trigger autophagy (Fig. 5H), suggesting that CPT1A's autophagy activation does not rely on its palmitoyltransferase activity. Subsequently, we aimed to identify the direct influence of ATG16L1 succination on autophagy activation. While mass spectrometry analysis did not reveal any potential sites, website analysis identified three possible succination sites on ATG16L1 (K101, K163, and K222). After mutating these sites to non-succinylation forms (K to R), we observed that the ATG16L1-K101R lost its capacity to activate autophagy (Fig. 5I). In conclusion, our results suggest that under chemotherapeutic drug treatment, CPT1A induces autophagy through

the succination of ATG16L1 at K101.

2.6. Etomoxir enhances chemosensitivity via inhibiting CPT1A-ATG16L1 mediated autophagy

Chemotherapeutic drugs are known to promote CPT1A-ATG16L1 mediated autophagy activation. Treating with 3-MA, an inhibitor of PI3K, is crucial in the formation and development of autophagosomes. 3-MA has been observed to reduce cisplatin resistance in hypopharyngeal carcinoma cells (HSCC) with overexpressed CPT1A (Fig. 6A). Etomoxir, a potent inhibitor of CPT1 (Bentebibel et al., 2006; Ceccarelli et al., 2011), can affect the chemotherapeutic sensitivity of hypopharyngeal carcinoma cells. An up-regulation of CPT1A could impair this sensitivity, while suppressing CPT1A might reverse the cells' drug resistance. Using etomoxir and cisplatin together has been shown to significantly kill hypopharyngeal carcinoma cells (Fig. 6B). To verify that etomoxir does not affect autophagy, we evaluated the LC3 and P62 levels with and without etomoxir. The results showed that etomoxir alone does not influence autophagy. However, when combined with cisplatin, it significantly inhibits the enhanced autophagy induced by cisplatin (Fig. 6C). Given the data obtained from *in vitro* models, we hypothesized that CPT1A could confer cisplatin resistance to HSCC cells by promoting autophagy. To test this, we inoculated FaDu cells subcutaneously in nude mice to observe tumor formation and size. As depicted in Fig. 6D, either etomoxir or cisplatin treatment marginally decreased tumor growth. However, combining etomoxir with cisplatin substantially reduced tumor growth (Fig. 6E). These findings suggest that inhibiting CPT1A might sensitise tumors to chemotherapy and that a combination of etomoxir and cisplatin could be a potential treatment strategy for HSCC.

3. Discussion

This study proposes a hypothetical mechanism whereby chemotherapeutic drugs induce CPT1A, which in turn promotes autophagy via the ATG12-ATG5-ATG16L1 complex in HSCC. CPT1A can bind to and succinylate ATG16L1 in human HSCC, leading to the formation of autophagosomes through the ATG12-ATG5-ATG16L1 complex and promoting autophagy activation. Consequently, by inducing autophagy, CPT1A plays a role in the survival of tumor cells and is associated with poor prognosis in HSCC patients. Our study is the first to reveal the molecular mechanism by which CPT1A acts as a key orchestrator of autophagosome formation and promotes autophagy through the ATG12-ATG5-ATG16L1 complex in HSCC. Importantly, CPT1A possesses not only succinyltransferase activities but also carnitine palmitoyl transferase activity. Although our report focuses solely on the succinyltransferase activity of CPT1A, it does not exclude a possible correlation between the succinyltransferase and carnitine palmitoyl transferase activities of CPT1A. The role of CPT1A in regulating chemoresistance in HSCC requires further investigation.

Notably, the role of autophagy in cancer is multifaceted. On one hand, autophagy triggered by chemotherapeutic drugs eliminates damaged organelles and macromolecules, thereby maintaining energy. This process enables tumor cells to resist stress and resume growth when conditions become favorable. On the other hand, prolonged over-activation of autophagy can stimulate autophagic cell death (ACD). Considering that

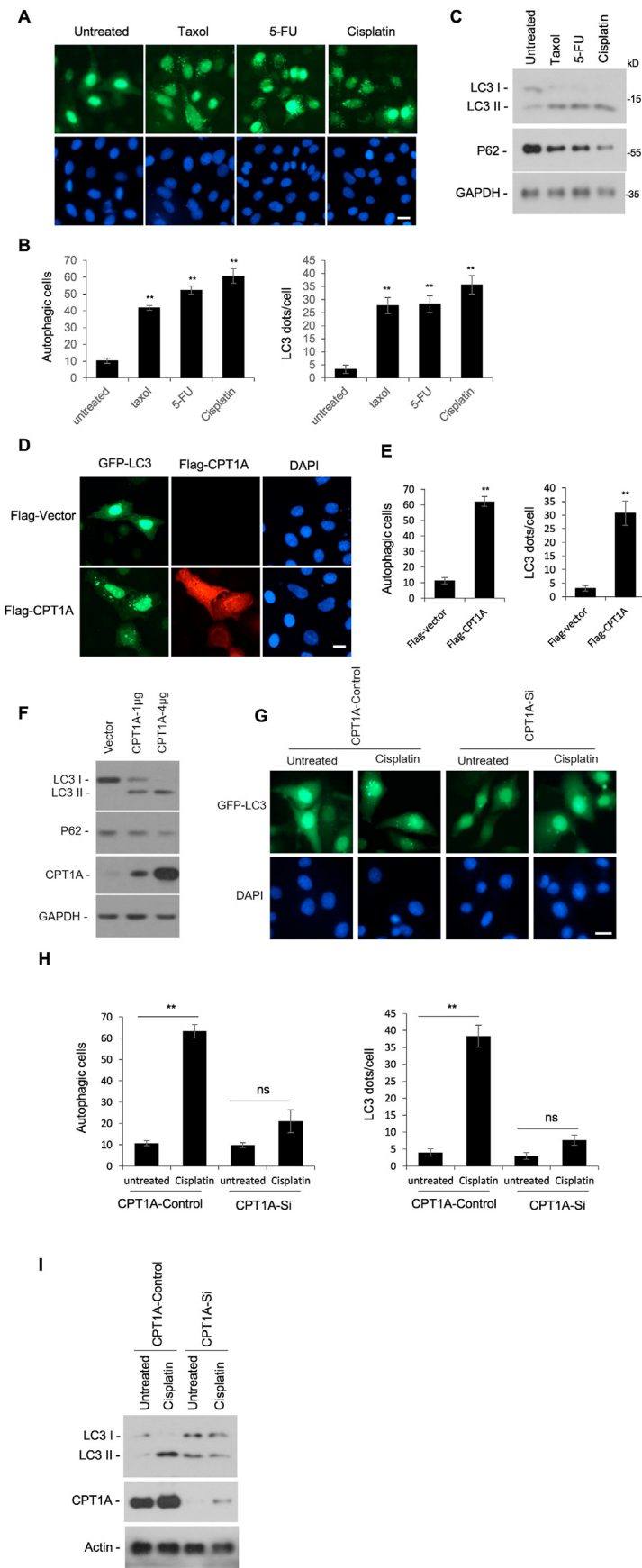


Fig. 3. CPT1A mediates autophagy under cisplatin treatment. (A) Fadu cells transfected with GFP-LC3 were treated with Taxol (10 nM), 5-FU (5 µM), and cisplatin (10 µM) for 12 h. GFP-LC3 was visualized by fluorescence microscopy (scale bar, 10 µm). (B) The percentages of GFP-LC3-positive cells with GFP-LC3 punctae and the GFP-LC3 punctae per cell in (A) were quantified. (C) Fadu cells were treated with Taxol (10 nM), 5-FU (5 µM), and cisplatin (10 µM) for 12 h. Cell lysates were then subjected to western blotting for LC3 and P62. (D) Flag-CPT1A and GFP-LC3 were co-transfected into Fadu cells. GFP-LC3 was visualized by fluorescence microscopy (scale bar, 10 µm). (E) The percentages of GFP-LC3-positive cells with GFP-LC3 punctae and the GFP-LC3 punctae per cell in (D) were quantified. (F) Fadu cells were transfected with CPT1A for 36 h. Cell lysates were then subjected to western blotting for LC3 and P62. (G–H) CPT1A knockdown and control cells transfected with GFP-LC3 were treated with cisplatin (10 µM) for 12 h. Representative immunofluorescence images showing GFP-LC3 dots are presented. The graphs represent the percentages of GFP-LC3 positive cells with GFP-LC3 punctae and the GFP-LC3 punctae per cell. (I) Immunoblot of LC3I/II in CPT1A control and knockdown cells treated with or without cisplatin (10 µM) for 12 h. Data represent the mean ± SD of three independent experiments. **p* < 0.05, ***p* < 0.01.

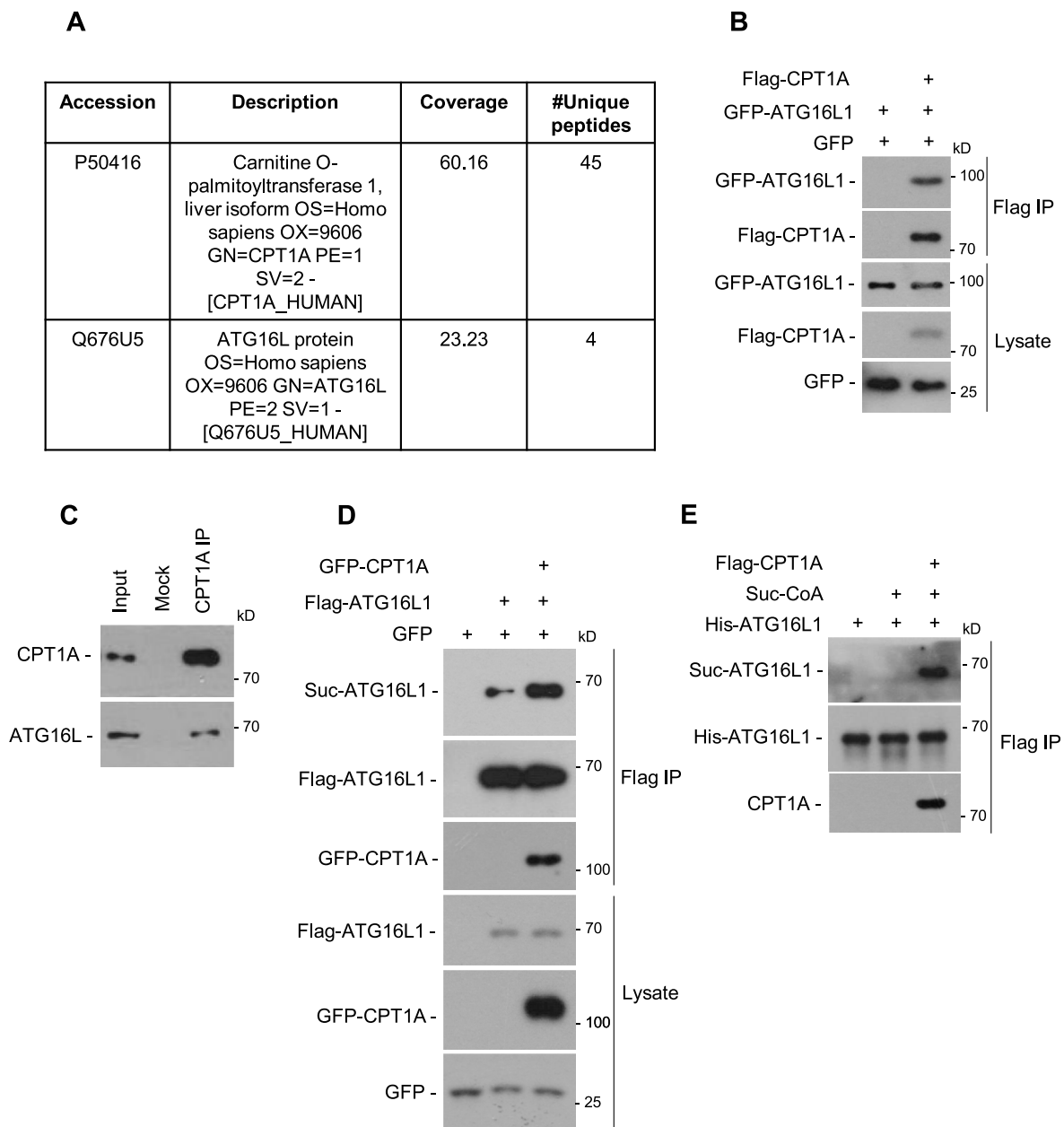


Fig. 4. CPT1A interacts with the autophagy-activated genes ATG16L1 and succinylates ATG16L1

(A) Mass spectrometry analysis was used to identify potential interacting proteins precipitated by CPT1A. (B) The interaction between exogenous CPT1A and ATG16L1 in 293T cells was explored. After transfection with Flag-CPT1A and GFP-ATG16L1 for 36 h, an immunoprecipitation assay using a Flag antibody was performed to determine ATG16L1 binding to CPT1A. Whole cell extracts were subjected to immunoprecipitation using the indicated antibodies. (C) Endogenous CPT1A in Fadu cells was precipitated using an anti-CPT1A antibody or IgG (mock IP). Co-precipitated ATG16L1 was detected using western blotting. (D) Following transfection with Flag-ATG16L1 and GFP-CPT1A for 36 h, immunoprecipitated Flag-ATG16L1 was immunoblotted with anti-pan-succinylated lysine and anti-Flag antibodies. Cell lysates were also immunoblotted for CPT1A. (E) His-ATG16L1 was expressed in *E. coli* and purified using His beads. CPT1A was precipitated from Flag-CPT1A-overexpressing 293T cells using FLAG-M2 beads and eluted with Flag peptide (100 μ g/ml). ATG16L1 protein was incubated with or without CPT1A in the presence or absence of succinyl-CoA as indicated. The reaction product was separated using SDS-PAGE and analyzed by western blotting.

apoptosis is often compromised in most cancer cells, ACD induced by anticancer drugs presents an attractive method for cancer treatment. Given that both the suppression and induction of autophagy could be advantageous for cancer therapy, the consideration of using autophagic inhibitors in research is necessary. Therefore, we incorporated 3-MA in our study and found that 3-MA treatment reduced cisplatin resistance in CPT1A-overexpressing HSCC cells. The regulation of cell growth, cell death, and drug resistance by targeting autophagy is a complex area of research focus in cancer therapy.

In summary, our current research demonstrates that CPT1A is highly expressed in HSCC patients. The high-level expression of CPT1A is correlated with an advanced T-stage and serves as a valuable predictor of poor prognosis in HSCC patients. In FaDu cells, the overexpression of CPT1A significantly promotes resistance to chemotherapeutic drugs, revealing its significant role in HSCC. This work provides novel insights into the roles of CPT1A in tumorigenesis and suggests that CPT1A could potentially be a therapeutic strategy for HSCC treatment.

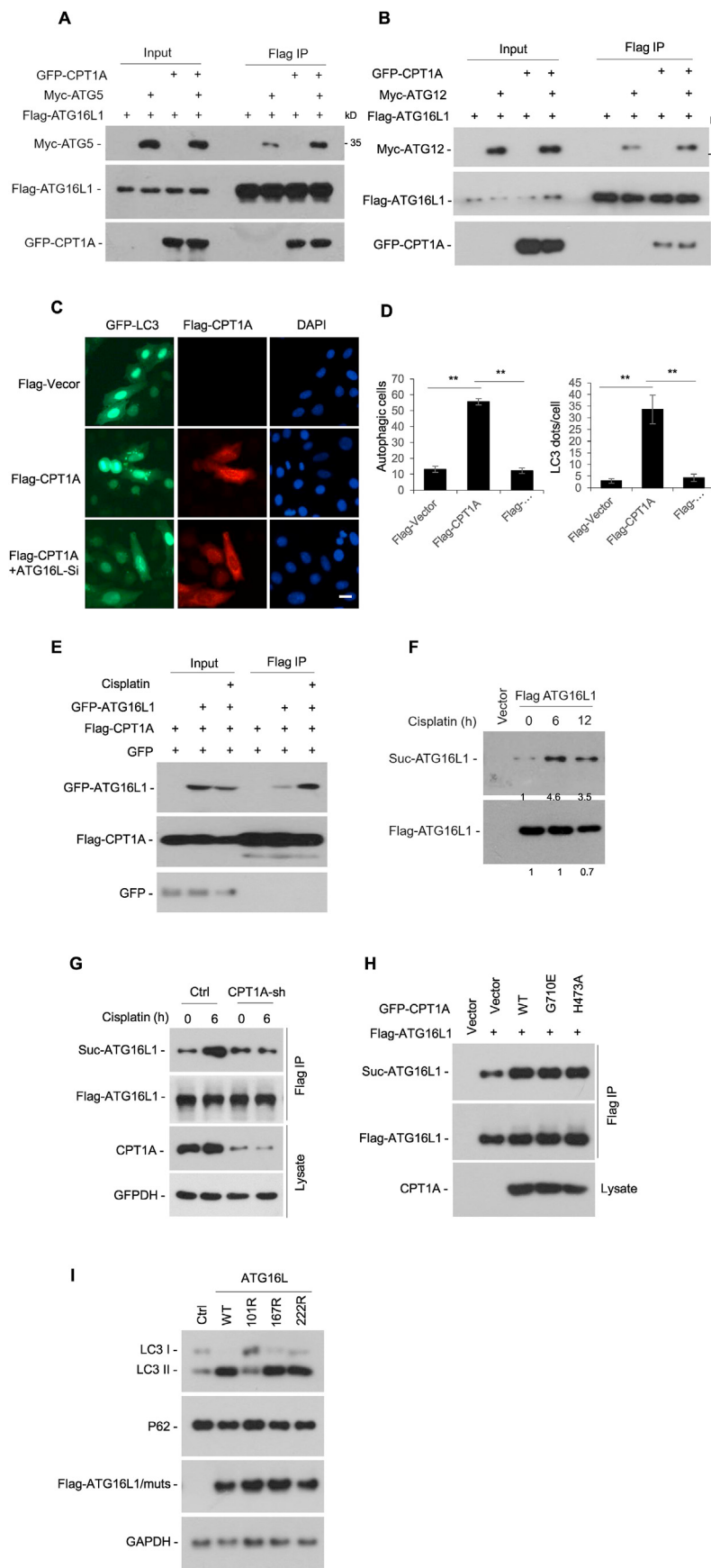


Fig. 5. CPT1A promotes autophagy through the ATG12-ATG5-ATG16L1 complex under chemotherapeutic drugs

(A-B) CPT1A facilitates the interaction between ATG5 and ATG16L1. Plasmids encoding GFP-CPT1A, Flag-ATG16L1, Myc-ATG5, or Myc-ATG12 were transfected into HEK293T cells. After 24 h, the cells were lysed. The interaction between ATG16L1 (immunoprecipitated using an anti-Flag antibody) and ATG5 was detected using an anti-Myc antibody. (C) Representative immunofluorescence images show GFP-LC3 staining in control cells, cells overexpressing CPT1A, and cells overexpressing CPT1A with ATG16L1 knocked down (scale bar, 10 μ m). (D) The graph represents the percentage of GFP-LC3 positive cells with GFP-LC3 punctae and the number of GFP-LC3 punctae per cell, as quantified from (C). (E) After treatment with cisplatin (10 μ M) for 12 h, 293T cells transfected with Flag-CPT1A and GFP-ATG16L1 were used to detect the CPT1A-ATG16L1 interaction through western blotting. (F) Fadu cells transfected with Flag-ATG16L1 were treated with cisplatin (10 μ M) for the indicated time periods. Immunoprecipitated Flag-ATG16L1 was immunoblotted with anti-pan-succinylated lysine and anti-Flag antibodies. (G) Flag-ATG16L1 was transfected into Fadu cells in which CPT1A was knocked down, and then treated with cisplatin (10 μ M) for 6 h. Immunoprecipitated Flag-ATG16L1 was immunoblotted with anti-pan-succinylated lysine and anti-Flag antibodies. The lysates were immunoblotted for CPT1A. (H) Flag-ATG16L1 and GFP-CPT1A-WT/G710E/H473A were transfected into Fadu cells. Immunoprecipitated Flag-ATG16L1 was immunoblotted with anti-pan-succinylated lysine and anti-Flag antibodies. The lysates were immunoblotted for CPT1A. (I) Flag-ATG16L1-WT and mutants (K101R/K167R/K222R) were transfected into Fadu cells and the cell lysates were immunoblotted for LC3 and P62. Data are presented as mean \pm SD from three independent experiments, ****** $p < 0.01$.

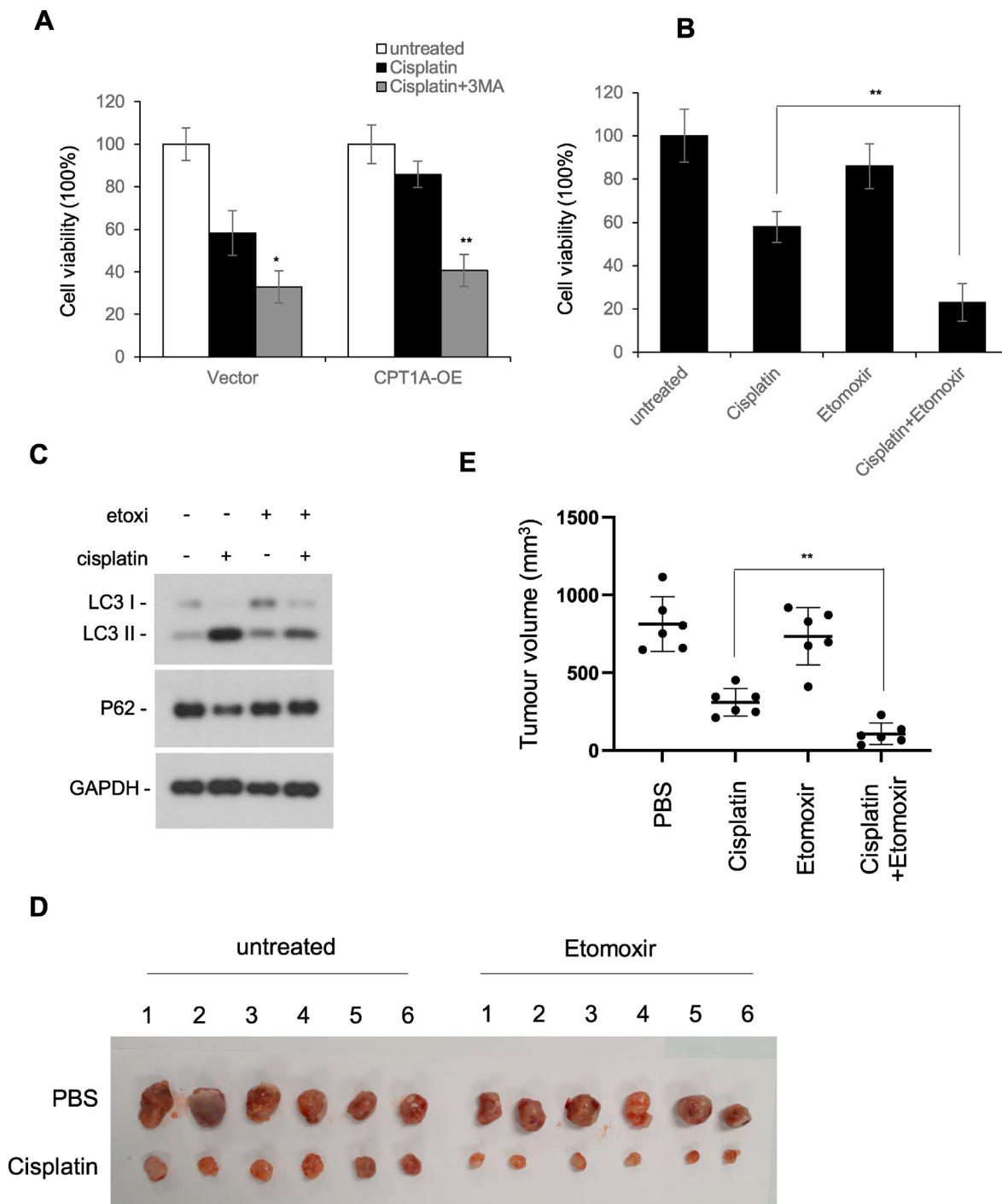


Fig. 6. Etomoxir enhances chemosensitivity via inhibiting CPT1A-ATG16L1 mediated autophagy

(A) Cisplatin resistance in hypopharyngeal carcinoma cell lines overexpressing CPT1A is reduced by 3-MA. FaDu cells stably transfected with either empty vectors or CPT1A plasmids were treated with 3-MA (5 mM) and cisplatin (10 μ M) for 48 h. Cell viability was subsequently assessed using the CCK8 assay. (B) The combined use of etomoxir and cisplatin significantly reduces the viability of hypopharyngeal carcinoma cells, as determined by the CCK8 assay. (C) FaDu cells were treated with cisplatin (10 μ M) either alone or in combination with etomoxir (1 μ M) for a duration of 12 h. The cell lysates were then immunoblotted for LC3 and P62. (D–E) The role of CPT1A in HSCC cell proliferation in vivo was explored using xenograft assays. A total of 3×10^6 FaDu cells were injected subcutaneously into athymic nude mice, which were then treated with etomoxir (20 mg/kg), cisplatin (4 mg/kg), or a combination of both. After a period of 30 days, the tumors were isolated and photographed (D), and their volumes were calculated (E). All data are presented as the mean \pm SD from three independent experiments. Statistical significance is indicated as * $p < 0.05$ and ** $p < 0.01$.

4. Methods

4.1. Patients and tissue specimens

Formalin-fixed paraffin-embedded (FFPE) samples from 19 patients

who were diagnosed with primary HSCC at Shanghai General Hospital (Shanghai, China) were collected. Paired tumor-adjacent normal tissue specimens were all available in 19 cases. All these samples were used for western blotting or immunohistochemical staining (IHC). Patients were classified according to TNM staging (American Joint Committee on

Cancer, 8th edition), and well documented with complete follow-ups for 5 years or until death. The study was approved by the Ethics Committee of Shanghai First People's Hospital and performed in accordance with the declaration of Helsinki Principles. Informed consent was obtained from each participant.

4.2. Animals

All mice used in this study are BALB/c nude mouse background and were bred in the specific-pathogen-free animal facility at Shanghai First People's Hospital. All the animal experiments were performed in accordance with protocols by the Animal Care and Use Committee at Shanghai First People's Hospital. All the surgeries were conducted under anesthesia and all efforts were made to minimize suffering of the animals.

4.3. In vivo tumor xenograft model

For the tumorigenesis assays, 4- to 6-week old female BALB/c nude mice were purchased from the animal facility of Shanghai First People's Hospital. Randomization was performed and animals were treated by an unblinded method. FaDu cells (2×10^6 suspended in 200 μ l PBS) were subcutaneously injected into each nude mouse. 14 days after implantation, etomoxir, cisplatin, or vehicle control (DMSO) were injected intratumorally every 3 days, six mice per group. The animals were euthanized when the tumor reached an endpoint size of ~ 1500 mm³, or ~ 4 weeks after implantation.

4.4. Cell culture and treatment with inhibitors

Human HNSCC cell line FaDu, Human embryonic kidney cell line 293T (HEK293T) cells were purchased from Shanghai Cell Bank of Chinese Academy of Sciences (Shanghai, China). The cells were cultured in Dulbecco's modified Eagle's medium (DMEM, Invitrogen) containing 10% fetal bovine serum (Invitrogen) and 1% penicillin/streptomycin at 37 °C in a humidified incubator containing 95% air and 5%CO₂. Cells were treated with inhibitors (Selleck, Shanghai, China) at indicated concentrations for 24 h. FaDu cells were seeded in a 6 well plate at a density of 10^5 cells per well and incubated overnight, then treated as indicated. Inhibitors were used at the indicated final concentrations (paclitaxel 1/10 IC50; fluorouracil 1/5 IC50; cisplatin 1/3 IC50). Cisplatin (Sigma, St. Louis, MO, USA) and fluorouracil (Sigma, St. Louis, MO, USA) were dissolved in 0.9% NaCl. Paclitaxel (Sigma, St. Louis, MO, USA) was dissolved in dimethylsulfoxide (DMSO).

4.5. In vitro cellular chemosensitivity to docetaxel, 5-fluorouracil, and cisplatin

To evaluate the cytotoxic effect of different concentrations of chemotherapeutic drugs, cells were seeded in 96-well plates at a density of 2×10^4 cells/well. After overnight incubation, the culture medium was replaced with fresh medium containing the indicated concentrations of chemotherapeutic drugs; a control set was included in which fresh medium alone was added, without any drugs. Cell viability was evaluated with a CCK-8 assay after 24, 36, and 48 h. The in vitro cell proliferation assay was carried out using a Cell Counting Kit-8 (Dojindo CK04, Shanghai, China) following the manufacturer's instructions. In brief, the cells were incubated for 30 min to 2 h after adding 10 μ l CCK8 solutions in 100 μ l medium, the absorbance at 450 nm was detected using a microplate reader.

4.6. Plasmid construction and transfection

C-terminal Flag-tagged expression for full-length CPT1A, ATG16L1, and ATG5 were constructed according to the standard protocol. All the plasmids were verified by sequencing before use (Sangon Biotech, Shanghai, China). The constructs were transfected into cell with PEI

(Polyscience) following the manufacturer's instructions.

The lentiviruses used in our study were produced by the standard protocol. Briefly, 5 μ g pMD2.G, 10 μ g PSPAX2, 10 μ g constructs for overexpression or knockdown of CPT1A were co-transfected into HEK293T cells in 100 mm cell culture dish with PEI (Polyscience). The lentivirus particles were obtained at 48 after transfection. Then, to get stably transfected cell lines, infected cells were selected with 2–4 μ g/mL of puromycin for 2 weeks. The knockdown and overexpression efficiency were confirmed by quantitative PCR (qPCR) and western blotting. The CPT1A shRNA was from sigma (targeting sequences: #1: GCTCTTAGA-CAAATCTATCTC, #2: GCCTTTGGTAAAGGAATCATC) were synthesized by Sangon Biotech (Shanghai, China).

4.7. RNA extraction and quantitative real-time PCR (qRT-PCR)

Total RNA was isolated from tissues or cell lines using TRIzol reagent (Takara). Total RNAs were reversely transcribed into cDNA by using RevertAid First Strand cDNA Synthesis Kit (Roche) according to the manufacturer's instructions. Synthesized cDNA was used for qRT-PCR in triplicate on a StepOnePlus™ Real-Time PCR System (Applied Biosystem). Using SYBR green master mix (Roche) Samples with low yield of RNA were pre-determined and excluded. Relative RNA levels of indicated genes were determined using the comparative 2^{- $\Delta\Delta$ CT} method and normalized to GAPDH. CPT1A sense primer: TCCAGTTGGCT-TATCGTGTG and anti-sense primer: CTAACGAGGGTTCGATCTTGG.

4.8. Immunohistochemistry (IHC)

We performed IHC experiments according to the standard method. The paraffin-embedded tissues were cut into 5 μ m thick slides. The sections were immunolabeled with anti-human CPT1A antibodies, followed by anti-mouse peroxidase kit labeling, respectively, according to the manufacturer's instructions.

For quantification analysis, three independent pathologists were blinded to the clinicopathologic information performed scoring using a light microscope to assess the IHC staining. The staining intensity of CPT1A was judged as follows: namely, 0, 1, 2, and 3, which were respectively defined as negative, weak staining, moderate staining, and strong staining. The percentage of positive cells was estimated as 0, 1, 2, 3, and 4 to indicate 0%–25%, 26%–50%, 51%–75%, and 76%–100% stained cells, respectively. The immunoreactive intensity score for each tissue was obtained by multiplying the staining value by the percentage category value, and finally the average score was calculated from scores of the three pathologists.

4.9. Immunofluorescence staining

The cell lines were seeded on glass-bottom culture dishes overnight. After that, the cells were fixed with 4% paraformaldehyde for 5 min and treated permeably by using 0.2% Triton X-100 for 10 min. The primary antibody were diluted in PBST (PBS+0.2%Triton X-100) and incubated with the cell lines for overnight at 4 °C. After three washed with PBST, the cell lines were incubated with Alexa 488-labeled anti-rabbit IgG (CST, 4412, 1:1000) and Alexa 647-labeled anti-mouse IgG (CST, 4410, 1:1000) also diluted in PBST for 30 min. Lastly, the cell lines were wash three times, mounted with DAPI containing mounting medium (Santa Cruz), and photographed by a confocal laser-scanning microscope (Carl Zeiss).

Paraffin sections (4 μ m thick) were first incubated in an oven at 60 °C for 2 h, then deparaffinized with xylene and rehydrated through gradient ethanol immersion. Antigen retrieval was processed by immersing slides in 0.01 M citrate buffer solution (pH 6.0) and boiling for 30 min to unmask the epitopes of paraffin-embedded samples. Primary antibodies against CPT1A were incubated overnight at 4 °C. For immunofluorescence cell staining, cells were fixed for 10 min in 4% PFA and blocked for 1 h with blocking buffer. The primary antibody was diluted in blocking

solution and incubated overnight at 4 °C. After washing, secondary antibodies were incubated for 1 h at room temperature. Then DAPI was counterstained for 5 min. Finally, the cells were mounted using anti fade mounting media. The mean fluorescence intensity and the percentage (0–100%) of positive cells were quantified by Image-Pro Plus from at least three raw, single-channel gray scale images, which were conducted at the same condition.

4.10. *In vitro* proliferation assay

For cell proliferation assay was carried out using a Cell Counting Kit-8 (Dojindo CK04, Shanghai, China) following the manufacturer's instructions. In brief, the cells were incubated for 30 min to 2 h after adding 10 µL CCK8 solutions into 100 µL medium. Then measure the absorbance at 450 nm using a microplate reader at indicated timepoints after seeding.

4.11. PAGE and immunoblot analysis

Cells were lysed with ice-colded SDS lysis buffer containing 125 mM Tris-HCl (pH 6.8), 4% SDS, 20% glycerol, and 0.004% bromphenol blue supplemented with complete protease cocktail (Roche, Switzerland), then boiled for 10 min. Protein concentrations were measured using the BCA Protein Assay Reagent (Pierce). Samples were diluted with the lysis buffer containing 1.28 M β-mercaptoethanol. Equal amounts of protein were loaded onto 8–10% SDS-polyacrylamide gels. Proteins were electrophoretically transferred to nitrocellulose membranes. The membranes were then blocked with 5% nonfat dry milk in PBS/Tween-20 (0.1%, v/v) for 2 h, then incubated with primary antibody for 2 h, followed by horseradish peroxidase-conjugated secondary antibody for 1 h.

4.12. Co-immunoprecipitation and western blotting

For co-immunoprecipitation assay, cells were lysed in IP lysis buffer (Beyotime) supplemented with complete protease cocktail (Roche, Switzerland). The cell lysates were incubated with the primary antibody for 6 h at 4 °C on a rotator. Protein A/G Magnetic beads (Beyotime) were then added and further incubated for 2 h at 4 °C on a rotator. After three washed with IP lysis buffer, protein complexes were released from Protein A/G Magnetic beads for 10 min in 2× SDS-PAGE loading buffer. Western blotting was conducted to detect protein expression or modification.

4.13. Mass spectrometry

Cells were lysed, and 10% of the cell lysate was used for input control, 90% of cell lysate was incubated with Flag antibody at 4 °C. Next day, protein A/G agarose beads (Beyotime) were added, and the incubation was further continued for 3 h at 4 °C. CPT1A-pulldown or rabbit IgG-pulldown proteins were loaded for 2× SDS-PAGE. After Coomassie brilliant blue staining, bands with strong intense signals were cut and digested. The resulting peptides were analyzed on the HPLC liquid system Dionex Ultimate 3000 (Thermo Scientific) coupled to a Dionex Trap column (100 µm × 2 cm X 5 µm) with in-house packed C18 column (75 µm × 15 cm X 3 µm), the mass of peptides was analyzed by maXis HD™-UHR-TOF mass spectrometer (Bruker). The spectra from mass spectrometry were automatically used for searching against the non-redundant International Protein Index human protein database (version 3.72) with the Bioworks browser (rev.3.1).

4.14. Statistical analysis

All sample sizes were large enough to satisfy statistical analyses that were analyzed using Graph Prime 8.0. All data were carried out using two-tailed Student's *t*-test, and the results are expressed as the mean ± standard deviation (SD) of three independent experiments. P

values are indicated in the Figure legends.

Author contributions

L.S., X.W., W.W. and L.C. performed most of the experiments; X.Y., L.S., W.W. and T. F. interpreted data and wrote the manuscript; G.F., C.H., S.X and Z.G. supervised the study and reviewed the manuscript. All authors read and approved the final manuscript.

Fundings

This work was supported by the National Natural Science Foundation of China (32070770, 82172921); Science and Technology Commission of Shanghai Municipality, China (20ZR1456000); Science and Technology Commission of Songjiang district, Shanghai (2020SJ284); Clinical Research Innovation Plan of Shanghai General Hospital (CTCCR-2021C13) and Shanghai “Rising Stars of Medical Talent” Youth Development Program -Youth Medical Talents - Clinical Pharmacist Program (SHWSRS(2020)_087).

Declaration of competing interest

The authors declare no competing interests.

References

- Bentebibel, A., et al. (2006). Novel effect of C75 on carnitine palmitoyltransferase I activity and palmitate oxidation. *Biochemistry*, 45(14), 4339–4350.
- Ceccarelli, S. M., et al. (2011). Carnitine palmitoyltransferase (CPT) modulators: A medicinal chemistry perspective on 35 Years of research. *Journal of Medicinal Chemistry*, 54(9), 3109–3152.
- Fujita, N., et al. (2008). The Atg16L complex specifies the site of LC3 lipidation for membrane biogenesis in autophagy. *Molecular Biology of the Cell*, 19(5), 2092–2100.
- Galluzzi, L., et al. (2015). Autophagy in malignant transformation and cancer progression. *The EMBO Journal*, 34(7), 856–880.
- Hanada, T., et al. (2007). The Atg12-Atg5 conjugate has a novel E3-like activity for protein lipidation in autophagy. *Journal of Biological Chemistry*, 282(52), 37298–37302.
- Hemelaar, J., et al. (2003). A single protease, Apg4B, is specific for the autophagy-related ubiquitin-like proteins GATE-16, MAP1-LC3, GABARAP, and Apg8L. *Journal of Biological Chemistry*, 278(51), 51841–51850.
- Holohan, C., et al. (2013). Cancer drug resistance: An evolving paradigm. *Nature Reviews Cancer*, 13(10), 714–726.
- Kurmi, K., et al. (2018). *Carnitine palmitoyltransferase 1A has a lysine succinyltransferase activity* (Vol. 22, pp. 1365–1373), 6.
- Kwon, D. I., & Miles, B. A. (2019). Hypopharyngeal carcinoma: Do you know your guidelines? *Head & Neck*, 41(3), 569–576.
- Lian, M., et al. (2017). In vivo gene expression profiling for chemosensitivity to docetaxel-cisplatin-5-FU (TPF) triplet regimen in laryngeal squamous cell carcinoma and the effect of TPF treatment on related gene expression in vitro. *Acta Oto-Laryngologica*, 137(7), 765–772.
- Luqmani, Y. A. (2005). Mechanisms of drug resistance in cancer chemotherapy. *Medical Principles and Practice*, 14(Suppl 1), 35–48.
- Mansoori, B., et al. (2017). The different mechanisms of cancer drug resistance: A brief review. *Advanced Pharmaceutical Bulletin*, 7(3), 339–348.
- Poillet-Perez, L., Sarry, J. E., & Joffre, C. (2021). Autophagy is a major metabolic regulator involved in cancer therapy resistance. *Cell Reports*, 36(7), Article 109528.
- Pointreau, Y., et al. (2009). Randomized trial of induction chemotherapy with cisplatin and 5-fluorouracil with or without docetaxel for larynx preservation. *Jnci-Journal of the National Cancer Institute*, 101(7), 498–506.
- Pu, J., et al. (2016). Mechanisms and functions of lysosome positioning. *Journal of Cell Science*, 129(23), 4329–4339.
- Qu, Q., et al. (2016). Fatty acid oxidation and carnitine palmitoyltransferase I: Emerging therapeutic targets in cancer. *Cell Death & Disease*, 7(5), e2226–e2226.
- Shao, H., et al. (2022). *Carnitine palmitoyltransferase 1A promotes mitochondrial fission and regulates autophagy by enhancing MFF succinylation in ovarian cancer*.
- Sui, X., et al. (2013). Autophagy and chemotherapy resistance: A promising therapeutic target for cancer treatment. *Cell Death & Disease*, 4(10), e838.
- Tan, Z., et al. (2018). Targeting CPT1A-mediated fatty acid oxidation sensitizes nasopharyngeal carcinoma to radiation therapy. *Theranostics*, 8(9), 2329–2347.
- Tan, Z., et al. (2021). Carnitine palmitoyl transferase 1A is a novel diagnostic and predictive biomarker for breast cancer. *BMC Cancer*, 21(1), 409.
- Tanida, I., et al. (2001). *The human homolog of Saccharomyces cerevisiae Apg7p is a protein-activating enzyme for multiple substrates including human Apg12p, GATE-16, GABARAP, and MAP-LC3* (Vol. 276, pp. 1701–1706), 3.
- Tanida, I., et al. (2002). Human Apg3p/Aut1p homologue is an authentic E2 enzyme for multiple substrates, GATE-16, GABARAP, and MAP-LC3, and facilitates the

- conjugation of hApg12p to hApg5p. *Journal of Biological Chemistry*, 277(16), 13739–13744.
- Vermorken, J. B., et al. (2007). Cisplatin, fluorouracil, and docetaxel in unresectable head and neck cancer. *New England Journal of Medicine*, 357(17), 1695–1704.
- Wang, J., et al. (2013). Aberrant expression of beclin-1 and LC3 correlates with poor prognosis of human hypopharyngeal squamous cell carcinoma. *PLoS One*, 8(7).
- Wang, C., et al. (2019). CPT1A-mediated succinylation of S100A10 increases human gastric cancer invasion. *Journal of Cellular and Molecular Medicine*, 23(1), 293–305.
- White, E. (2015). The role for autophagy in cancer. *Journal of Clinical Investigation*, 125(1), 42–46.
- White, E., & DiPaola, R. S. (2009). The double-edged sword of autophagy modulation in cancer. *Clinical Cancer Research*, 15(17), 5308–5316.
- Wilson, T. R., Longley, D. B., & Johnston, P. G. (2006). Chemoresistance in solid tumours. *Annals of Oncology*, 17(Suppl 10), x315–x324.
- Xiao, X., et al. (2018). HSP90AA1-mediated autophagy promotes drug resistance in osteosarcoma. *Journal of Experimental & Clinical Cancer Research*, 37(1), 201.
- Xiong, J. (2018). Fatty acid oxidation in cell fate determination. *Trends in Biochemical Sciences*, 43(11), 854–857.
- Xu, J. L., et al. (2020). The role of autophagy in gastric cancer chemoresistance: Friend or foe? *Frontiers in Cell and Developmental Biology*, 8, Article 621428.
- Yan, Y., et al. (2016). Targeting autophagy to sensitive glioma to temozolomide treatment. *Journal of Experimental & Clinical Cancer Research*, 35(1), 23.